

## Response Letter (For Referee 1)

### Comment from Referee 1:

“In this work, Liu et al. studied the formation of sulfate on mixed mineral dust particles and found a synergistic effect between  $\text{TiO}_2$  and carbonate in promoting sulfate formation upon illumination. They proposed a novel mechanism in which carbonate radical ( $\bullet\text{CO}_3^-$ ) was considered as an important intermediate. This  $\bullet\text{CO}_3^-$  was assumed to oxidize  $\text{SO}_3^{2-}$  to  $\bullet\text{SO}_3^-$  and then promote sulfate formation. Lots of methods were used to prove the existence of  $\bullet\text{CO}_3^-$  and its interaction with other species in this reaction system. Furthermore, analysis of samples collected in field observation and quantum chemical calculation were also used to show this synergistic effect between  $\text{TiO}_2$  and carbonate in promoting sulfate formation in the atmosphere. The formation mechanism of sulfate is an important research topic in atmospheric chemistry as well as the occurrence of high concentration of fine particles during haze episodes. This work provided a new and interesting perspective for synergistic effect in the formation of atmospheric sulfate aerosol. However, the flaws in the hypothesis of reaction mechanism make its scientific and environmental significance questionable. In addition, the manuscript is not well organized and a little hard to read. So, I think it may not be accepted in current version.”

### Author general reply:

Thanks for your valuable suggestions, which greatly helped us to improve the manuscript. According to your comments, we have noted the flaws and shortcomings in the argument, especially for the controversial role of carbonate ions in sulfate formation under irradiation. We thus supplied a series of experiments to further improve and modify the reaction scheme proposed in the previous submission, and revised the manuscript to provide more convincing explanations to the readers. Besides, the role of superoxide radical ions, more precisely the sink of photo-generated electrons and its contribution to sulfate formation relative to carbonate radical ions have been discussed in the revised version of the manuscript. Further, we supplied a more detailed discussion to connect each paragraph on a common string of reasoning, which will guide the readers to capture the whole picture of the manuscript and to get the take-home message. We carefully consider all your comments posted to the previous version of the manuscript, and the detailed point-by-point revisions are presented as follows.

### Main concerns.

**Q1-A:** It is not reasonable to exclude the buffering effect of carbonate in promoting the formation of sulfate. The results that  $\text{CaCO}_3$  did not promote the formation of sulfate under dark conditions (Page 6 line 155) can not extend to confirm its effect in promoting sulfate formation under illumination. It has been well known that the conversion of  $\text{SO}_2$  to S(VI) hardly happen under ambient conditions without strong oxidants or illumination. On the other hand, several recent studies reported that mineral dust photochemistry can induce the formation  $\text{H}_2\text{SO}_4$  (PNAS, 2012, 109, 208842–20847; EST, 2021, 55, 14, 9784-9793). In the present study, it seems the increase in sulfate concentration under illumination condition is most likely due to the enhanced condensation or neutralization of  $\text{H}_2\text{SO}_4$  in the presence of  $\text{CaCO}_3$  or carbonates.

**Response to Q<sub>1</sub>-A:** Thanks for your question. We note that dark experiments may not fully rule out the possibility where photo-generated oxidants accelerate sulfate formation due to the favorable neutralization over alkaline surfaces. Therefore, several supplementary experiments were performed to validate our findings, as shown below:

### 1. SO<sub>2</sub> oxidation over TiO<sub>2</sub>+CaCO<sub>3</sub> mixture and TiO<sub>2</sub>+CaO mixture

Indeed, it remains puzzle for the role of carbonate salt in sulfate formation either by favoring neutralization of H<sub>2</sub>SO<sub>4</sub> on alkaline surfaces or by serving as the precursor of active CO<sub>3</sub><sup>-</sup> to trigger the fast sulfate formation as we proposed in this work. Therefore, we employed two types of mixtures TiO<sub>2</sub>+CaCO<sub>3</sub> and TiO<sub>2</sub>+CaO. According to the EDS mapping analysis of relevant component contents of the Arizona test dust (ATD) (Table S1), the mass fraction ratio of TiO<sub>2</sub> to CaCO<sub>3</sub>/CaO are thus fixed at 1:7 to mimic the synergistic effect that is likely to take place over the authentic dust particles. In the dark experiments, both TiO<sub>2</sub>+CaO and TiO<sub>2</sub>+CaCO<sub>3</sub> almost yield identical concentration levels of sulfite and sulfate, indicating that they show similar surface properties, e.g. alkalinity and the number of surface sites. Once irradiated, TiO<sub>2</sub>+CaCO<sub>3</sub> particles produce nearly two times of sulfate than TiO<sub>2</sub>+CaO particles, along with a sharp decrease of S(IV) species on the surface of TiO<sub>2</sub>+CaCO<sub>3</sub> surfaces. This result confirms the existence of the formation of active intermediates that drive the fast SO<sub>2</sub> oxidation when carbonate salt is presented. In addition, the total sulfur content, i.e. S(IV)+S(VI), in TiO<sub>2</sub>+CaCO<sub>3</sub> particles is quite higher than that in TiO<sub>2</sub>+CaO particles upon irradiation, whereas they are almost identical in the dark experiments. Consequently, the difference between two mixtures regarding sulfate yield under illumination can be mainly attributed to the formation of additional reaction channels that have been not previously considered. Another plausible explanation is that carbonate radical ions promote sulfate formation by forming the carbonate radical in the gas phase (see results in Fig. R3) and thus yield more secondary sulfate aerosol in the gas phase. Part of them will then condense back onto particle surfaces to increase total sulfate yield.

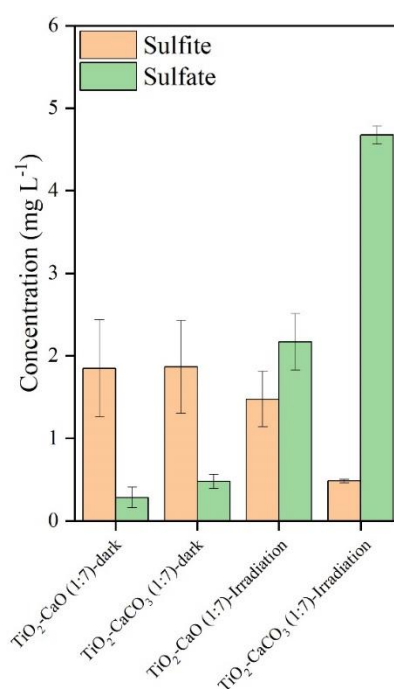


**Fig. R1.** Sulfate and sulfite concentration quantified by IC on mineral dust proxies after exposure

to gaseous SO<sub>2</sub> under irradiation or dark for 20 min. Reaction conditions: RH = 30 %, Light intensity (I) = 30 mW cm<sup>-2</sup>, Total flow rate = 52.5 mL min<sup>-1</sup> and SO<sub>2</sub> = 2.21×10<sup>14</sup> molecules cm<sup>-3</sup>.

***Detailed correction in the manuscript:***

*“While great discrepancies in sulfate yield between dark and irradiation experiments, it remains unclear for the role of carbonate salt in promoting sulfate formation. There is a prevailing view that neutralization of H<sub>2</sub>SO<sub>4</sub> accounts for rapid SO<sub>2</sub> oxidation over carbonate salt particles, which needs careful consideration. Following this speculation, two types of mixtures TiO<sub>2</sub>-CaCO<sub>3</sub> and TiO<sub>2</sub>-CaO were employed. In the dark condition (Fig. S3), both TiO<sub>2</sub>-CaO and TiO<sub>2</sub>-CaCO<sub>3</sub> almost yield an identical concentration of sulfite and sulfate as they are likely to present similar physical and chemical properties, e.g. surface pH and neutralization capability. Once irradiated, TiO<sub>2</sub>-CaCO<sub>3</sub> particles produce nearly two times of sulfate than TiO<sub>2</sub>-CaO particles, along with a sharp decrease of S(IV) species on the surface of TiO<sub>2</sub>-CaCO<sub>3</sub> surfaces (see additional discussion in the supplementary text 2). These results allow us to assert that the carbonate-containing system contains another important mechanism for sulfate generation beyond the production of an alkaline environment.” (Main Text, Page 4, Line 108-117)*

**2. Observation of strengthened oxidation capability in carbonate-containing TiO<sub>2</sub> suspension**

To validate the formation of carbonate radical strengthening oxidative capacity of carbonate-containing TiO<sub>2</sub> particles under irradiation, aniline is used as probe molecular, which is reported to have a high reaction rate with carbonate radical ions ( $k_{\cdot\text{OH},\text{aniline}} = 6.5 \times 10^9 \text{ M}^{-1}\text{s}^{-1}$ ) (Samuni et al., 2002). In Fig. R2, a difference between “air + irradiation” system and “TiO<sub>2</sub> + air + irradiation” system mainly comes from the contribution of hydroxyl radical instead of from other intermediates (e.g. superoxide radical, see discussion in the next subsection “Determination of gas-phase ROS production in the flow-cell reactor”). When carbonate ions are introduced into TiO<sub>2</sub> suspension, leaving the pH of the reaction system at 11, the removal rate of aniline is evidently increased. We noted that increasing pH favors the formation rate of ·OH radical, which has been well verified in numerous works (Chavadej et al., 2008; Kansal et al., 2008; Tang and An, 1995). To examine the net contribution of carbonate radical ions to the increased oxidation capability of the carbonate-containing TiO<sub>2</sub> system beyond the increased pH environment, we performed the reference experiment using “TiO<sub>2</sub>+ air +NaOH” reaction system. In detail, an adequate amount of NaOH was added into TiO<sub>2</sub> suspension to have the pH of TiO<sub>2</sub> suspension identical to that of TiO<sub>2</sub>+Na<sub>2</sub>CO<sub>3</sub>. Indeed, it shows a higher removal rate than “TiO<sub>2</sub>+ air” but a lower removal rate than “TiO<sub>2</sub>+ Na<sub>2</sub>CO<sub>3</sub>+air”. It seems to suggest that higher alkaline carbonate salt favors in promoting sulfate formation in part due to the increased OH yield. Nevertheless, one should note that carbonate radical ions are predominant species in a relatively alkaline environment in the presence of carbonate since the carbonate ion is an excellent ·OH scavenger.

The previous work (Sun et al., 2016) shows that adding 0.1 M of NaHCO<sub>3</sub> into the UV/H<sub>2</sub>O<sub>2</sub> system (H<sub>2</sub>O<sub>2</sub> = 0.3 mM) were sufficient to suppress ·OH concentration to around 10<sup>-15</sup> M, creating a carbonate radical dominated reaction system ( $[\text{CO}_3^{\cdot-}] = 8.64 \times 10^{-12} \text{ M}$ ). In our supplementary experiments, 0.2 M of Na<sub>2</sub>CO<sub>3</sub> was employed, and the reaction rate of CO<sub>3</sub><sup>2-</sup> with ·OH is over one order of magnitude higher than that with HCO<sub>3</sub><sup>-</sup>, thus giving rise to carbonate radical being the substitute of hydroxyl radical in the reaction system and responsible for enhanced aniline degradation.

Overall, when (bi)carbonate ions are present, carbonate radical ions that are enriched on the surface of TiO<sub>2</sub> increase the overall oxidation capability of TiO<sub>2</sub> particles. Besides, the increase of pH favors the production of CO<sub>3</sub><sup>•-</sup>, further strengthening the oxidation capability of dust particles.

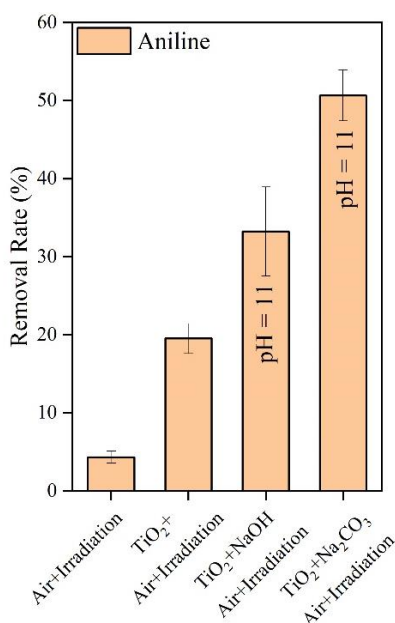


**Fig. R2.** The removal rate of aniline after exposure to air flow under irradiation in the absence and presence of mineral dust particles for 300 seconds. Reaction conditions: RH = 30 %, Light intensity (I) = 30 mW cm<sup>-2</sup>, Total flow rate = 52.5 mL min<sup>-1</sup>. Noting that an adequate amount of NaOH was introduced into TiO<sub>2</sub> suspension system to achieve a pH environment condition comparable to that of TiO<sub>2</sub>-Na<sub>2</sub>CO<sub>3</sub> suspension system.

***Detailed correction in the manuscript:***

*“A promoted degradation of aniline in TiO<sub>2</sub> suspension due to presence of carbonate ions presents additional evidence of the formation of active CO<sub>3</sub><sup>•-</sup> ions and strengthened oxidative capability of TiO<sub>2</sub> (Fig. S11, see more discussion in supplementary text 4).” (Main Text, Page 10, Line 246-248)*

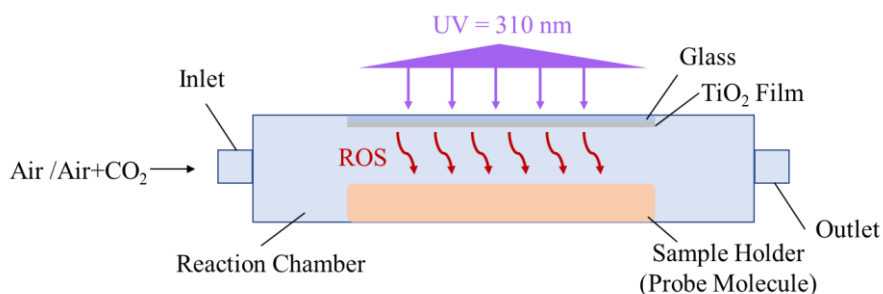
*“This is plausible since the carbonate ions are excellent ·OH scavenger, and CO<sub>3</sub><sup>•-</sup> become predominant species at a relatively strong alkaline aqueous-like environment in the presence of carbonate salt. This is supported by the previous work (Sun et al., 2016), in which adding 0.1 M of NaHCO<sub>3</sub> into the UV/H<sub>2</sub>O<sub>2</sub> system (H<sub>2</sub>O<sub>2</sub>=0.3 mM) were sufficient to suppress ·OH concentration to around 10<sup>-15</sup> M, creating a carbonate radical dominated reaction system ([CO<sub>3</sub><sup>•-</sup>] = 8.64 × 10<sup>-12</sup> M). In our supplementary experiments (Fig. S11), 0.2 M of carbonate salt was employed, and the reaction rate of CO<sub>3</sub><sup>2-</sup> with ·OH is nearly two orders of magnitude higher than that of HCO<sub>3</sub><sup>-</sup>, thus giving rise to carbonate radical being the substitute of hydroxyl radical in the reaction. The above results suggest that ·OH is a major contributor to sulfate yield on TiO<sub>2</sub> particles in the absence of carbonate ions while CO<sub>3</sub><sup>•-</sup> ions dominate SO<sub>2</sub> oxidation over carbonate-containing dust particles upon irradiation.” (Main Text, Page 10, Line 255-264)*

**3. Determination of gas-phase ROS production in the flow-cell reactor**

Dust particles are reported to eject the radical ions from the surface under solar light irradiation, showing a non-negligible contribution to sulfate aerosol formation (Chen et al., 2021; Dupart et al., 2012). Over 400 ppm of CO<sub>2</sub> is universal in the atmosphere, and it can form (bi)carbonate ions once enters into the atmospheric aqueous media such as aerosol water, cloud droplets as well as fog environment. Bi(carbonate) ions readily react with hydroxyl radical ions to form carbonate radical ions. Following this line of reasoning, we attempt to monitor the plausible ROS species that are released from dust particles when bi(carbonate) ions are involved.

To measure the concentration of ROS released from TiO<sub>2</sub> particles in various reaction systems, an experimental approach using the probe molecule compound aniline was applied in this study. This is because aniline is reported to react rapidly with ·OH radicals and CO<sub>3</sub><sup>·-</sup> radicals, which are also evidenced to be two major active ROS species that are responsible for the SO<sub>2</sub> oxidation over mineral dust particles. The method applied in this study was almost implemented as the same to that of the previous study (Behrman, 2018), with slight modification. Briefly, the degradation rate of aniline in various reaction systems were monitored through High-Performance Liquid Chromatography (HPLC, LC-10AD, SHIMADZU, Japan). A Zorbax SB C18 (4.6 mm × 150 mm, 5 μm) reverse phase column at 25 °C was used with a UV detector at 236 nm to measure the aniline concentration. The mobile phase consisted of acetonitrile/water = 55:45 (V/V) with a flow rate of 1 mL/min.

TiO<sub>2</sub> suspension (5 mg TiO<sub>2</sub> per 100 uL deionized water) was deposited onto the glass substrate (0.13-0.17 mm in thickness) using a pipette and then dried in the oven for 10 min to obtain a TiO<sub>2</sub>-coated film. Dilute aniline solution, using 67 mM phosphate buffer solution (pH = 7.0), was prepared and placed below the TiO<sub>2</sub>-coated film, with an intervening gap between TiO<sub>2</sub> film and solution surface around 2 mm. This short distance allows gaseous ROS (·OH radicals and CO<sub>3</sub><sup>·-</sup> radicals, etc) to diffuse and react with aniline molecular (None, 2013).



**Scheme R1.** The schematic of flow-cell reaction chamber for gaseous ROS determination.

In the reaction system containing TiO<sub>2</sub> film upon irradiation (the UV wavelength = 310 nm) in the presence of humidified air (RH = 30 %), when operated in a continuous mode, the overall degradation rate of probe molecular in the presence of TiO<sub>2</sub> film can be described by Eq. **R1** (Wang et al., 2004):

$$k_{\text{obs}} = \frac{d[\text{An}]}{dt} = r_A + r_U + r_{\text{ROS}} = r_A + r_U + k_{\text{ROS+AN}}[\text{ROS}][\text{An}] \quad [\text{R1}]$$

Where  $k_{\text{obs}}$  is the observed degradation rate of aniline,  $[\text{An}]$  is the concentration of aniline, denoted as  $[\text{An}]$  hereafter, and  $r_A$ ,  $r_U$ ,  $k_{\text{ROS}}$  stand for aniline removal rates resulting from air stripping, UV photolysis, ROS oxidation.  $k_{\text{ROS+AN}}$  are the overall second-order reaction rate constants for An with ROS.

Reference experiments without the introduction of ROS were also conducted to measure  $r_A+r_U$  in each reaction system, e.g. An+TiO<sub>2</sub>+Air+Irradiation, Aniline+TiO<sub>2</sub>+N<sub>2</sub>+Irradiation, etc. Upon irradiation, the dust proxy TiO<sub>2</sub> produces hole-electron pairs, further forming ·OH radicals and superoxide radicals (O<sub>2</sub><sup>·-</sup>) in the presence of absorbed water and oxygen molecules. Thus, a supplementary experiment using N<sub>2</sub> was adopted to investigate the role of O<sub>2</sub><sup>·-</sup> in consuming aniline. As shown in Fig. R3, a slight change in the degradation rate of aniline after stripping oxygen from the air, indicating that O<sub>2</sub><sup>·-</sup> shows quite a smaller contribution than ·OH. This result agrees well with the finding reported by Durán et al. (Duran et al., 2019), where removal of O<sub>2</sub><sup>·-</sup> by adding benzoquinone (BQ) into TiO<sub>2</sub> suspension results in the negligible change of An degradation rate.

Taken above, ·OH radicals are tentatively assumed to be the only active ROS that accounts for the An degradation. Hence, the maximum steady concentration of ·OH radicals can be given by the following equation:

$$-\frac{d[\text{An}]}{dt}=k_{\text{exp}}[\text{An}]=k_{\cdot\text{OH},\text{An}}[\cdot\text{OH}]_{\text{ss-max}}[\text{An}] \quad \text{[R2]}$$

Integration of Eq. R2 yields

$$-\ln \frac{[\text{An}]_t}{[\text{An}]_0}=k_{\text{exp}}t \quad \text{[R3]}$$

$$k_{\text{exp}}=k_{\cdot\text{OH},\text{An}}[\cdot\text{OH}]_{\text{ss-max}} \quad \text{[R4]}$$

Together with the reported second-order rate constant ( $k_{\cdot\text{OH},\text{An}} = 6.5 \times 10^9 \text{ M}^{-1}\text{s}^{-1}$ ) (Samuni et al., 2002), the steady-state OH radical concentration  $[\cdot\text{OH}]_{\text{ss-max}}$  in buffered An solution can be calculated from Eq R2. The observed degradation rate constant of  $k_{\text{exp}}$  can be obtained from the slope of the semi-log plot of An degradation as shown in Eq R3. The maximum steady-state concentration of ·OH radical ions supplied by partition processes between gas phase and solid-liquid phases (humified dust particles) was thus estimated to be  $2.15 \times 10^{-15} \text{ M}$  for the TiO<sub>2</sub>+Air system.

When CO<sub>2</sub> (400 ppm, atmospheric relevant concentration) is introduced into the flow-cell chamber, an increased degradation rate of An is seen, which can be attributed to the generation of active carbonate radical ions. Similar to the method we adopted for the estimation of  $[\cdot\text{OH}]_{\text{ss-max}}$ , reference experiments were conducted to determine the rates for air stripping and UV photolysis processes in the TiO<sub>2</sub>+Air+CO<sub>2</sub> system. In the next step, we quenched the hydroxyl radicals by adding tertiary butanol (TBA). In the extreme case, assuming that all hydroxyl radical ions were fully trapped by absorbed and dissolved HCO<sub>3</sub><sup>-</sup>/CO<sub>3</sub><sup>2-</sup> over TiO<sub>2</sub> film and gaseous water molecular in the humidified air flow, the maximum steady-state CO<sub>3</sub><sup>·-</sup> radical concentration was determined to be  $1.39 \times 10^{-13} \text{ M}$  for TiO<sub>2</sub>+Air+CO<sub>2</sub> system, matching well with the earlier study where the concentration of carbonate radical can be two orders of magnitudes than ·OH over the water surface (Sulzberger et al., 1997b).

The above supplementary results suggest that the photochemistry that CO<sub>3</sub><sup>·-</sup> radical increases sulfate formation. This finding broadens the previous prevailing view that acceleration of SO<sub>2</sub> oxidation over the carbonate salt is merely due to the favorable neutralization of H<sub>2</sub>SO<sub>4</sub> over alkaline surfaces. To be important, upon irradiation active component TiO<sub>2</sub> in mineral dust will produce carbonate radical in the gas phase when the atmospherically relevant concentration of CO<sub>2</sub> is presented, therefore potential promoting sulfate aerosol formation in the atmosphere. Overall, it could be deduced that carbonate radical ions strengthen the oxidative capability of dust particles TiO<sub>2</sub>, and consequently accelerate SO<sub>2</sub> oxidation.



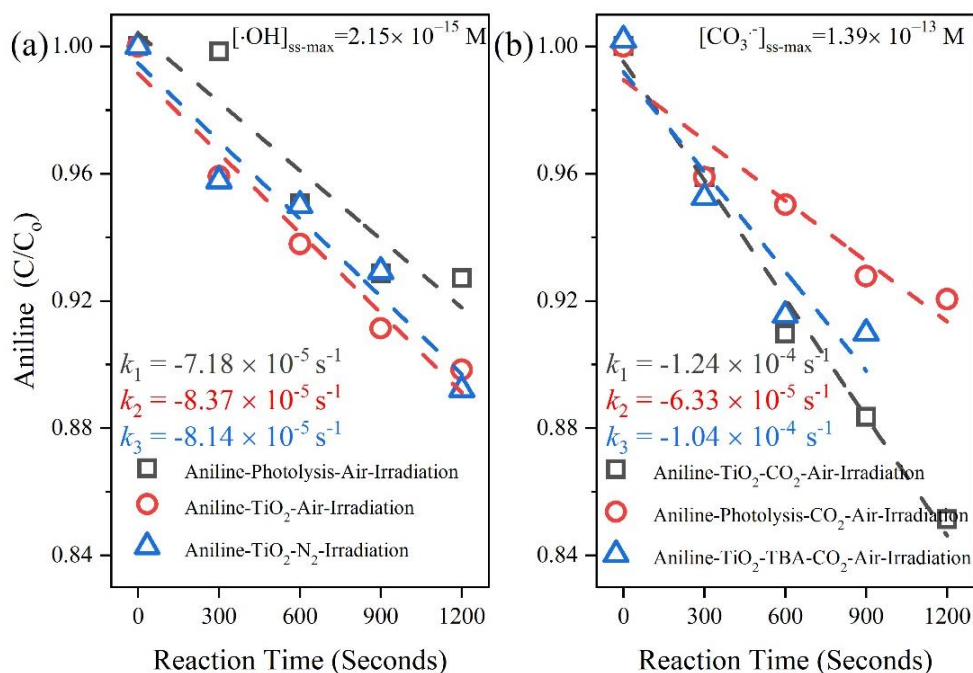
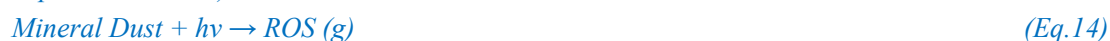


**Fig. R3.** The degradation rate of aniline after exposure to air flow under irradiation in the absence (a) and presence (b) of CO<sub>2</sub> over mineral dust proxy particles TiO<sub>2</sub> as function of the reaction time. Reaction conditions: RH = 30 %, Light intensity (I) = 30 mW cm<sup>-2</sup>, Total flow rate = 52.5 mL min<sup>-1</sup>.

**Detailed correction in the manuscript:**

“Additionally, dust particles are reported to eject the radical ions from the surface under solar light irradiation, showing a non-negligible contribution to sulfate aerosol formation (Chen et al., 2021; Dupart et al., 2012), as described as:



Where ROS (g) stands for the active intermediates in the gas phase. Over 400 ppm of CO<sub>2</sub> is in the atmosphere, and it is expected to form (bi)carbonate ions once enters into the atmospheric aqueous media such as aerosol water, cloud droplets as well as fog environment. Bi(carbonate) ions are then prone to react with hydroxyl radical ions to form carbonate radical ions. Following this line of reasoning, we attempt to monitor the plausible gas ROS species that are formed in the presence of CO<sub>2</sub> (see detailed discussion about the measurement approach and experimental setup in supplementary text 7 and Fig. S16).

When CO<sub>2</sub> (atmospheric relevant concentration) is introduced into the homemade flow-cell chamber, with the intervening gap between TiO<sub>2</sub>-coated film and probe molecule solution fixing at nearly 2 mm, and a short distance of which allows possible gaseous ROS to diffuse and react with aniline molecular (None, 2013). An increased degradation rate of aniline was seen, which can be attributed to the generation of active carbonate radical ions (Fig. S17). The maximum concentration of steady-state CO<sub>3</sub><sup>·-</sup> radical ions supplied by partition processes between gas phase and solid-liquid phases (humidified dust particles) was determined to be 1.39 × 10<sup>-13</sup> M for the TiO<sub>2</sub>+Air+CO<sub>2</sub> system, which is over one order of magnitudes higher than that of ·OH for the TiO<sub>2</sub>+Air+system (2.15 × 10<sup>-15</sup> M). This observation matches with the earlier study where the concentration of carbonate radical

can be two orders of magnitudes than  $\cdot\text{OH}$  over the water surface (Sulzberger et al., 1997a).

The above results suggest that the photochemistry that involves carbonate ions, more precisely  $\text{CO}_3^{\cdot-}$  radical, increases sulfate formation. This finding broadens the prevailing view that acceleration of  $\text{SO}_2$  oxidation over the carbonate salt is merely due to the favorable neutralization of  $\text{H}_2\text{SO}_4$  over an alkaline surface. To be important, upon irradiation active component  $\text{TiO}_2$  in mineral dust produce carbonate radical in the gas phase when  $\text{CO}_3^{\cdot-}$  precursor  $\text{CO}_2$  is presented, therefore potentially promoting sulfate aerosol formation in the atmosphere. Overall, it could be deduced that carbonate radical ions strengthen the oxidative capability of  $\text{TiO}_2$ -containing mineral dust particles, and consequently accelerates  $\text{SO}_2$  oxidation.” [\(Main Text, Page 14, Line 365-387\)](#)

**Q1-B:** I think the  $\text{CO}_2+\text{SO}_2$  experiments may not rule out the buffering effect of carbonate effect in  $\text{TiO}_2+\text{CaCO}_3$  system since the enhancement effect of  $\text{CO}_2$  is significantly lower than that on  $\text{CaCO}_3$ . Moreover, why  $\text{SO}_2$  concentration in Figure 2 is quite lower than those in Figure 1? And could you show the IR peaks due to  $\text{CO}_2$  adsorption? Did their intensities change during the photooxidation of  $\text{SO}_2$ ?

**Response to Q1-B:** Thanks for your question. As reported by the previous study (Czapski et al., 1999), the reaction rate of hydroxyl radical with carbonate ions is nearly one order magnitude higher than that with bicarbonate ions. Therefore, carbonate salt can produce much more carbonate radical ions than  $\text{CO}_2$  does, and consequently promote  $\text{SO}_2$  oxidation more evidently.

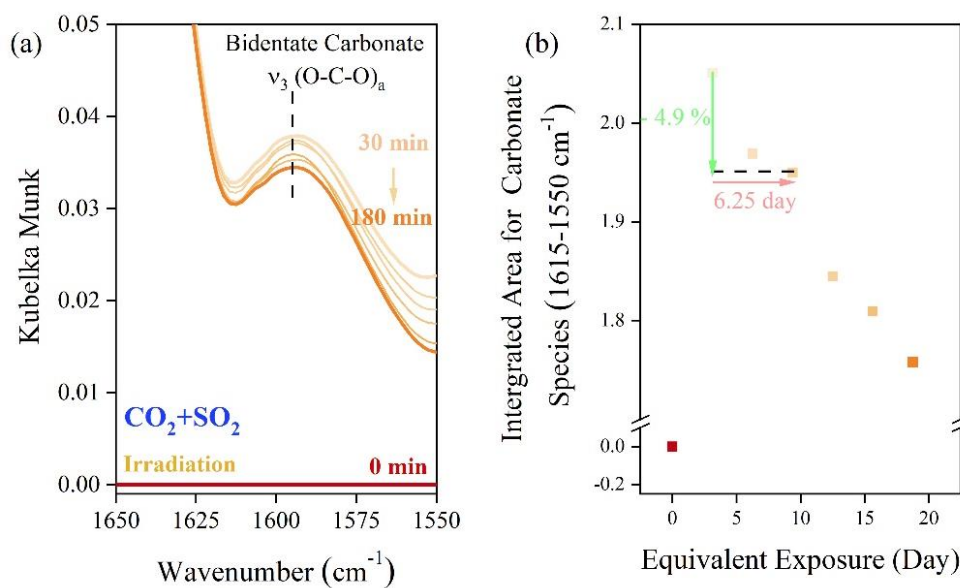


**Fig. R4.** Time-resolved DRIFTS of carbonate products over  $\text{TiO}_2$  particles after exposure to  $\text{SO}_2/\text{N}_2+\text{O}_2$  in the presence of  $\text{CO}_2$  upon irradiation. Reaction conditions:  $\text{RH} = 30\%$ , Light intensity ( $I$ ) =  $30 \text{ mW cm}^{-2}$ , total flow rate =  $52.5 \text{ mL min}^{-1}$  and  $\text{SO}_2 = 7.37 \times 10^{13} \text{ molecules cm}^{-3}$ .

In Figure 1, we employed the HRTEM technique to analyze the sulfate distribution on the  $\text{TiO}_2$ - $\text{CaCO}_3$  particles to elucidate the reaction mechanism for the increased sulfate yield. While this benefits us to figure out the scheme behind the observation, one limitation appears for this methodology, that is a relatively high sulfate concentration required to overcome its relatively low detection limit. To address this issue, we elevated the  $\text{SO}_2$  concentration for heterogeneous reaction



to monitor sulfate feature in HETEM images, i.e. high resolution with lattice fringes, and we also carefully consider the influence of SO<sub>2</sub> concentration on the reaction kinetics by examining the reaction order of SO<sub>2</sub> on the dust particles. Within the range of 400-20000 ppb SO<sub>2</sub> (Fig. S10), the heterogeneous reaction of SO<sub>2</sub> on mineral dust particles follows the pseudo-first-order. Therefore, despite some inconsistency of SO<sub>2</sub> concentration applied in different reaction systems, it would not give fundamental influence on our findings and observations where the increased sulfate formation comes from the formation of carbonate radical ions due to the synergistic effect between TiO<sub>2</sub> and CaCO<sub>3</sub>.

Time-resolved IR bands assigned to CO<sub>2</sub> adsorption over TiO<sub>2</sub> particle surface during the heterogeneous photo-oxidation of SO<sub>2</sub> have been presented in Fig. R4. For TiO<sub>2</sub> dust particles, the absorption at 1533 cm<sup>-1</sup> is specifically assigned to the vibrational modes of the adsorbed monodentate carbonate (Baltrusaitis et al., 2011; Nanayakkara et al., 2015). There is a decrease in the intensity in the O-C=O region as heterogeneous reaction proceeds during 180 min. Following Jiang's work (Jiang et al., 2019), we introduced the concept of "equivalent exposure time" in analyzing the DRIFTS data. The "equivalent exposure time" refers to the theoretical exposure time of SO<sub>2</sub> at an atmospherically-relevant concentration that TiO<sub>2</sub> and TiO<sub>2</sub>-CaCO<sub>3</sub> particles are exposed to. The equivalent exposure time is calculated by multiplying the reaction time in the lab with the scale factor, which is the ratio of SO<sub>2</sub> concentration applied in DRIFTS experiments to SO<sub>2</sub> concentration possible in the atmospherically-relevant condition (20 ppb). Nevertheless, considering a large SO<sub>2</sub> concentration gap between the lab simulations and field observations, direct extrapolation of equivalent exposure time into such low SO<sub>2</sub> concentration may not be appropriate. Therefore, the reaction kinetics of SO<sub>2</sub> on mineral dust particles TiO<sub>2</sub> was investigated, and it is evidenced to follow the pseudo-first-order in the SO<sub>2</sub> concentration range of 400 ppb-20000 ppb, which covers all SO<sub>2</sub> concentrations applied in this study. While a concentration gap between lab studies and field observation remains, we tentatively assume this gap has a marginal impact on the kinetics considered. On this basis, we plotted integrated areas of the IR peak at 1615-1550 cm<sup>-1</sup> versus equivalent exposure time (Fig. R4b).

The mean lifetime of mineral dust particles in the atmosphere is nearly one week (Bauer and Koch, 2005). In our study, nearly one week of equivalent exposure of atmospheric SO<sub>2</sub> gives rise to the reduction of 4.9 % of carbonate species. Therefore, this moderate consumption of absorbed carbonate slightly affects the abundance of carbonate ions and the production of CO<sub>3</sub><sup>-</sup>.

**Q<sub>2</sub>:** Consistency and comparability of experimental system. The heterogeneous reactions of SO<sub>2</sub> were studied on mineral particles while some characterization experiments for supporting evidences were conducted in solutions. Although some water layers may be formed on mineral dust particle surface at 30 % RH, however, this situation may far from the liquid state. So, it is unreasonable to assume that all reaction mechanisms are ionic reactions in liquid phase.

**Response to Q<sub>2</sub>:** Thanks for your question. We understand your concern about the consistency issue for reaction systems in the adsorbed water layer and aqueous media. On one hand, the experiments for carbonate radical detection were conducted in solution, which is unavoidable since it is a requirement for the nanosecond transient absorption technique and ESR measurements. On the other hand, at a sufficiently low RH condition (normally below 10 % RH), water readily dissociates on the surface of metal oxide under ambient atmospheric conditions, where metal oxide surface is terminated by hydroxyl groups (Cwiertny et al., 2008). In this case, SO<sub>2</sub> oxidation over dust particles

is dominated by the heterogenous pathway, where the resulting hydroxyl groups capture  $\text{SO}_2$  in the gas phase first and then stabilize it to adsorbed  $\text{S(IV)}_{\text{ad}}$  over dust surfaces. Afterward,  $\text{S(IV)}_{\text{ad}}$  will be oxidized by oxidants in the atmosphere or photo-induced active intermediates produced from the dust surface upon irradiation.

As the RH increases beyond 10 % - 15 %, multilayer water coverage occurs, reaching approximately two monolayers at RH of 30 % (Mogili et al., 2006). Under these circumstances, the amount of water adsorbed onto the surface of the dust particles is believed to be sufficiently large that it is liquid-like in its physical and chemical properties (Cwiertny et al., 2008) (Peters and Ewing, 1997). In this work, heterogenous  $\text{SO}_2$  oxidation over mineral dust proxies proceeds at the RH of 30 %, and two water layers absorb on dust particles. Thus, radical ions are expected to play a key role in fast  $\text{SO}_2$  oxidation. Taken above, the mechanism studies performed in solution phase are persuasive to some extent.

***Detailed correction in the manuscript:***

*“At a sufficiently low RH condition (normally below 10 % RH), water readily dissociates on the surface of metal oxide under ambient atmospheric conditions, where metal oxide surface is terminated by hydroxyl groups that hydrogen bond to adsorbed water molecules (Cwiertny et al., 2008). In this case,  $\text{SO}_2$  oxidation over dust particles is dominated by the heterogenous pathway, where the resulting hydroxyl groups capture  $\text{SO}_2$  in the gas phase first and then stabilize it as adsorbed  $\text{S(IV)}_{\text{ad}}$ . Afterward,  $\text{S(IV)}_{\text{ad}}$  will be oxidized by oxidants in the atmosphere or photo-induced active intermediates produced from the dust surface upon irradiation. As the RH increases beyond 10 % -15 %, multilayer water coverage occurs, reaching approximately two monolayers at RH of 30 % (Mogili et al., 2006). Under these circumstances, the amount of water adsorbed onto the surface of the dust particles is believed to be sufficiently large that it is liquid-like in its physical and chemical properties (Cwiertny et al., 2008) (Peters and Ewing, 1997). In this work, heterogenous  $\text{SO}_2$  oxidation over mineral dust proxies proceeds at the RH of 30 %, and two water layers absorb on dust particles. Thus, radical ions are expected to play a key role in fast  $\text{SO}_2$  oxidation and mechanism studies performed in solution phase are persuasive to some extent.”*

**(Main Text, Page 9, Line 222-233)**

**Q3-A:** Mechanism: Firstly, only hole was consumed which resulted in the formation of  $\cdot\text{OH}$  and  $\cdot\text{CO}_3^-$  (eq 2 and 3). However, the consumption of photogenerated electron is not mentioned. According to eq 5-8,  $\text{O}_2$  is the key oxidant for the oxidation of  $\text{SO}_3^{2-}$  to sulfate. However, the content of  $\text{O}_2$  in solution is limited due to its low solubility if aqueous reactions were assumed. In addition,  $\text{O}_2$  can react with photogenerated electron to form  $\text{O}_2^-$  and then oxidize  $\text{SO}_3^{2-}$  on particles surface. The authors need to compare the effect of these two processes on the formation of sulfate.

**Response to Q3-A:**

**The sink of  $\text{O}_2$  and role of  $\text{O}_2^-$**

Thank you for your valuable comments. We considered the sink of photo-generated electrons and the role of superoxide radical ions ( $\text{O}_2^-$ ) in sulfate formation. In addition, we supplied the  $\cdot\text{OH}$  scavenger experiment to monitor the contribution of  $\text{O}_2^-$  and  $\cdot\text{OH}$  to sulfate formation over  $\text{TiO}_2$  particles. *p*-benzoquinone is a commonly-used  $\text{O}_2^-$  scavenger for trapping the  $\text{O}_2^-$  radical ions (Yan et al., 2018). Our supplementary data shows that adding an excess amount of *p*-benzoquinone into

TiO<sub>2</sub> particles reduces the sulfate yield by 32 % along with the appearance of sulfite ions found over TiO<sub>2</sub> particles upon exposure to SO<sub>2</sub>. On the other hand, Tertiary Butyl Alcohol (TBA), ·OH scavenger, sharply decreases the yield of sulfate on TiO<sub>2</sub> surface by nearly 70 %, with sulfite ions being the dominant sulfur species. Notably, the decrease in sulfate yield by around 30 % in the presence of O<sub>2</sub><sup>-</sup> scavenger *p*-benzoquinone is almost complementary to that added with ·OH scavenger using TBA (70 %), pointing toward a minor sulfate formation pathway contributed by O<sub>2</sub><sup>-</sup> relative to the major pathway by CO<sub>3</sub><sup>-</sup> when carbonate ions are presented to efficiently to capture ·OH ions. Nevertheless, O<sub>2</sub><sup>-</sup> plays a non-negligible role in sulfate formation and should be incorporated to give a whole picture of the reaction scheme in triggering sulfate formation on the surface of TiO<sub>2</sub> particles. We have added this pathway into the main text.

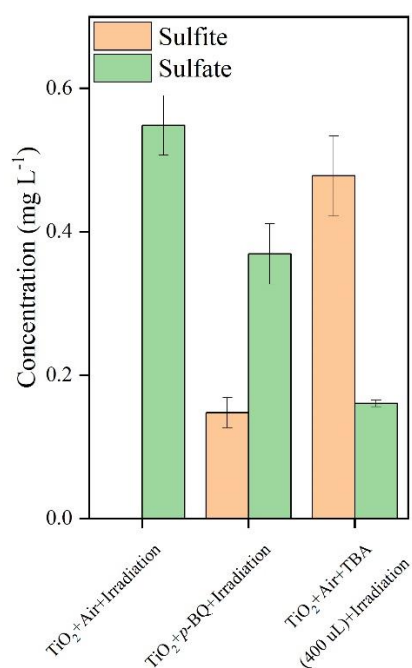


**Fig. R5.** Determination of sulfite and sulfate concentration after exposure to air flow under irradiation in the absence and presence of mineral dust particles for 20 min. Reaction conditions: RH = 30 %, Light intensity (I) = 30 mW cm<sup>-2</sup>, Total flow rate = 52.5 mL min<sup>-1</sup>.

**Detailed correction in the manuscript:**

*“In addition to the pathway launched by photo-generated holes, we also considered the sink of photo-generated electrons. In our reaction system, O<sub>2</sub> is believed to be an electron trap and produce the superoxide radical ions (O<sub>2</sub><sup>-</sup>), which is reported to play a non-negligible role in sulfate formation (Shang et al., 2010a) and should be taken into account to give a whole picture of reaction scheme in triggering sulfate formation on the surface of TiO<sub>2</sub>-containing mineral dust particles. *p*-benzoquinone is a commonly-used O<sub>2</sub><sup>-</sup> scavenger for trapping the O<sub>2</sub><sup>-</sup> radical ions (Yan et al., 2018). Our supplementary data shows that adding an excess amount of *p*-benzoquinone into TiO<sub>2</sub> particles reduces the sulfate yield by 32 % along with the appearance of sulfite ions over TiO<sub>2</sub> particles upon exposure of SO<sub>2</sub> (Fig.S12). Interestingly, the decrease in sulfate yield by around 30 % in the presence of O<sub>2</sub><sup>-</sup> scavenger *p*-benzoquinone is almost complementary to that added with ·OH scavenger using TBA (70 %), pointing toward a minor sulfate formation pathway contributed by O<sub>2</sub><sup>-</sup> relative to the major pathway by CO<sub>3</sub><sup>-</sup> when carbonate ions are presented to efficiently capture ·OH ions.*”

Following Shang's work (Shang et al., 2010a),  $O_2^{\cdot-}$  involved  $SO_2$  oxidation can be given as Eqs. 11-13:

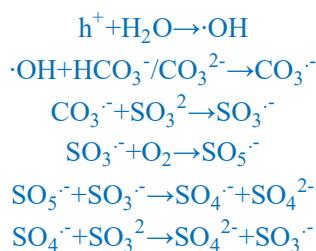


Where intermediates  $SO_3$  formed via the interaction between  $SO_2$  and  $O_2^{\cdot-}$  subsequently couple with water molecules to produce sulfate species as a final product." **(Main Text, Page 14-, Line 337-352)**

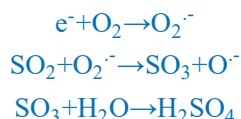
### Oxygen supply and consumption:

In addition to the consideration of the role of  $O_2^{\cdot-}$  in sulfate formation over  $TiO_2$  particles. We supplied estimation of oxygen consumption rates and oxygen supply rates in the reaction systems considered in this study. When (bi)carbonate ions are introduced into the reaction, they serve the excellent  $\cdot OH$  scavenger to form  $CO_3^{\cdot-}$ , leaving two major active intermediates  $O_2^{\cdot-}$  and  $CO_3^{\cdot-}$  responsible for fast sulfate formation.

For  $CO_3^{\cdot-}$  pathway:



For  $O_2^{\cdot-}$  pathway:



As we discussed above, the relative contribution of  $CO_3^{\cdot-}$  and  $O_2^{\cdot-}$  to overall sulfate formation over  $TiO_2$  particles could be assumed to be 0.7 and 0.3, respectively. Together with the major  $SO_2$  oxidation reaction channel considered above, one may note that 1 mole of oxygen contributes to 1.7 moles of sulfate, and  $H_2O$  provides an additional oxygen source compensating for the oxygen deficit. Given the measured  $SO_2$  uptake coefficient in the DRIFTS chamber, the sulfate formation rates are thus determined to be  $0.33 \mu M s^{-1} m^{-2}$  for geo surface of  $TiO_2$  particles, known as the upper limit of uptake capability, corresponding to the maximum oxygen consumption rate of nearly  $0.19 \mu M s^{-1} m^{-2}$ . For  $TiO_2 + CaCO_3$  particles, the sulfate formation rate is  $2.01 \mu M s^{-1} m^{-2}$ . We applied the relation (1 mole of oxygen  $\sim$  1.7 moles of sulfate) for calculating the oxygen consumption rate in the  $TiO_2 + CaCO_3$  system. This operation leads to a conservative estimation of oxygen consumption rate since the relative contribution of carbonate radical ions to sulfate formation are expected to be even more predominant in the " $TiO_2 + CaCO_3 + Air$ " system (1 mole of oxygen  $\sim$  2 moles of sulfate) than that in " $TiO_2 + CO_2 + Air$ " system (1 mole of oxygen  $\sim$  1 mole of sulfate). Therefore, the oxygen consumption rate is not likely to exceed  $1.18 \mu M s^{-1} m^{-2}$ .

We further considered the oxygen supply capability over water layers attached to the dust particles. A steady-state of gas diffusion is described as a state where the diffusion flux density  $J_s$ , stays

constant and by integration from 0 to  $l$ . Fick's first law can be expressed in the following form (Nguyen et al., 1992):

$$J_s = -D \frac{\Delta C}{l} \quad [R5]$$

where,  $\Delta C$  is the concentration difference between saturation and the system at a given time, and  $D$  the mass transfer coefficient (0.021 millimeters<sup>2</sup>/s), and  $l$  the distance between water layers with gradient oxygen concentration. At RH = 30 %, nearly two aqueous-like water layers are believed to adsorb onto the dust particle surface (Mogili et al., 2006) (Peters and Ewing, 1997), and around 0.3 nm, known as the typical thickness feature for mono water layer (Ali et al., 2015; Gao et al., 2020; Ruiz-Agudo et al., 2013), and 0.6 nm is thus adopted for  $l$ . For degassed single water layer devoid of O<sub>2</sub> in our system, the flux of O<sub>2</sub> supplied across the two aqueous-like water layers is at a rate of 17.08 M s<sup>-1</sup> m<sup>-2</sup>, which is several orders of magnitude higher than that of oxygen consumption determined for both “TiO<sub>2</sub>+CO<sub>2</sub>+Air” and “TiO<sub>2</sub>+CaCO<sub>3</sub>” systems. Therefore, oxygen is sufficient in the reaction, allowing the considered chain reactions to continually proceed.

***Detailed correction in the manuscript:***

*“However, we noted that the insufficient O<sub>2</sub> supply in aqueous media may be an underlying constraint to the proposed CO<sub>3</sub><sup>-</sup>-initiated SO<sub>2</sub> oxidation pathway. Hence, we estimated both oxygen consumption and supply rates, and oxygen supply flux can be several orders of magnitude larger than corresponding consumption flux (see detailed discussion in the supplementary text 5). Therefore, oxygen is sufficient in the reaction, allowing the considered chain reactions to continually proceed.”*

**(Main Text, Page 12, Line 300-304)**

**Q<sub>3</sub>-B-1:** Secondly, according to eq 6-8 (in eq 7, SO<sub>4</sub> should be SO<sub>4</sub><sup>2-</sup>?)

**Response to Q<sub>3</sub>-B-1:** Thanks for your careful review and it should be SO<sub>4</sub><sup>2-</sup>, which has been revised and highlighted in the current version of the manuscript.

**Q<sub>3</sub>-B-2:** It seems that the oxidation of SO<sub>3</sub><sup>2-</sup> by O<sub>2</sub> could be a catalytic reaction while •SO<sub>3</sub><sup>-</sup> acted as catalyst. If so, the amounts of sulfate formed through photooxidation on TiO<sub>2</sub> should be the same (at least close to) in the presence of carbonates and CO<sub>2</sub> since •CO<sub>3</sub><sup>-</sup> only contribute to the formation of •SO<sub>3</sub><sup>-</sup>. Is it?

**Response to Q<sub>3</sub>-B-2:** Carbonate ions capture •OH more efficiently than bicarbonate ions (more than one order of magnitude). Consequently, carbonate ions can yield more CO<sub>3</sub><sup>-</sup> than bicarbonate ions do. Carbonate salt and CO<sub>2</sub> are known to dissociate into (bi)carbonate ions in the aqueous medium, in which carbonate ions are dominant in the aqueous system containing carbonate salt while bicarbonate ions are major species in the CO<sub>2</sub>-aerated solution. Therefore, over humidified dust particles, carbonate radical ions are expected to be enriched in “TiO<sub>2</sub>+carbonate salt” scenario, more abundant than in “TiO<sub>2</sub>+CO<sub>2</sub>” one.

Besides, DFT calculation provides theoretical evidence that carbonate radical ions decrease the energy barrier for SO<sub>3</sub><sup>-</sup>-formation, and its reaction with SO<sub>3</sub><sup>2-</sup> is thus faster than that with hydroxyl radical (Fig. 4 b and c). Considering this, CO<sub>2</sub> and carbonate ions serves as a precursor of CO<sub>3</sub><sup>-</sup>, and thus increases sulfate yield. Therefore, sulfate yield over TiO<sub>2</sub> particles in the presence of CO<sub>2</sub> and carbonate ions is higher than that over pristine TiO<sub>2</sub>.

**Q3-C:** Thirdly, what's the pH effect on the reaction? As seen in eq 3 and 4, only the reaction of  $\cdot\text{OH}$  with  $\text{HCO}_3^-/\text{CO}_3^{2-}$  was considered. What's about the reactions between  $\text{H}^+$  and  $\text{HCO}_3^-/\text{CO}_3^{2-}$ ? As the oxidation of  $\text{SO}_2$  or sulfite increased, the pH should decrease and then affect  $\text{HCO}_3^-/\text{CO}_3^{2-}$ .

**Response to Q3-C:** pH ( $\text{H}^+$  concentration) is an important factor within the aqueous chemical reaction process. Yet so far adjusting the pH ( $\text{H}^+$  concentration) of particle surfaces is quite tough, and exploring the role of dust surface pH ( $\text{H}^+$  concentration) in the reactivity of  $\text{CO}_3^-$  is not easily achieved. Notwithstanding, as we discussed in the section "Q1-2. Observation of carbonate radical formed in carbonate-containing  $\text{TiO}_2$  suspension", the increase of pH in  $\text{TiO}_2$  suspension was observed to promote the production of  $\text{CO}_3^-$ , further strengthening the oxidation capability of dust particles. In contrast, decreasing pH is expected to reduce the yield of  $\text{CO}_3^-$  since the reaction rate of  $\text{CO}_3^{2-}$  with  $\cdot\text{OH}$  is lower than that with  $\text{HCO}_3^-$ . On this basis, we then examined whether the pH of the mineral dust surface can be sustained to maintain fast  $\text{SO}_2$  oxidation triggered by sufficient  $\text{CO}_3^-$  in the typical lifespan of mineral dust after accumulation of sulfate production. Considering this, we thus plotted the heterogeneous sulfate production over  $\text{TiO}_2$  and  $\text{TiO}_2+\text{CaCO}_3$  particles versus equivalent exposure time (Fig. R6).

The heterogeneous reaction of  $\text{SO}_2$  on  $\text{TiO}_2$  in the presence of  $\text{CO}_2$  as well as on  $\text{TiO}_2+\text{CaCO}_3$  mixtures was investigated by *in situ* DRIFTS technique. Similar to the  $\text{TiO}_2+\text{Air}+\text{CO}_2$  system, we also plotted the heterogeneous sulfate production over  $\text{TiO}_2$  and  $\text{TiO}_2+\text{CaCO}_3$  particles versus equivalent exposure time assuming that the atmospherically relevant concentration of  $\text{SO}_2$  is 20 ppb (Fig. R6). The equivalent exposure time determined for these two sets of experiments is across one day to nearly two weeks. Clearly, the sulfate yield builds up steadily during the two-week equivalent exposure time, suggesting that the regime of  $\text{CO}_3^-$  initiated  $\text{SO}_2$  oxidation over  $\text{TiO}_2$  and  $\text{TiO}_2-\text{CaCO}_3$  particles is slightly affected by the decrease of surface pH due to the accumulation of sulfate production over the course of equivalent exposure time. In the atmosphere, the lifetime of typical mineral dust particles ranges from several days to weeks (Bauer and Koch, 2005), and the equivalent exposure time considered in this study (nearly 2 weeks) falls right within the characteristic lifespan range of mineral dust particles. This leads us to deduce that pH variation due to persistent growth of sulfate during the reaction shows a negligible effect on  $\text{CO}_3^-$  initiated  $\text{SO}_2$  oxidation channel proposed in this work.



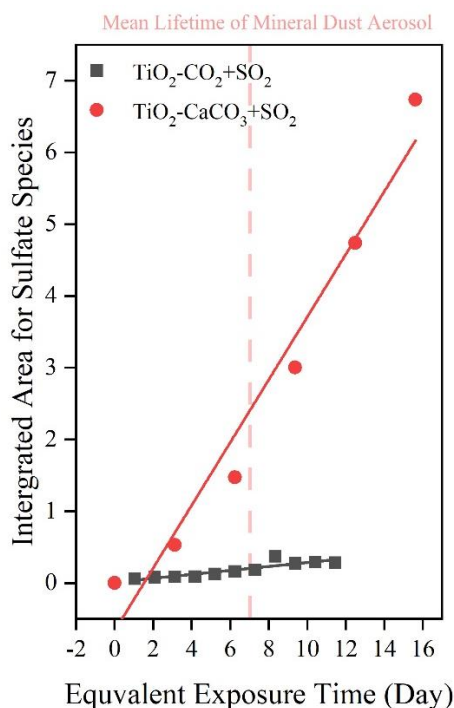


**Fig. R6.** *In situ* DRIFTS of S(IV) and S(VI) species on TiO<sub>2</sub> and TiO<sub>2</sub>+CaCO<sub>3</sub> mixtures (wt./wt. = 50/50) upon irradiation as function of equivalent exposure time. Reaction conditions: RH = 30 %, Light intensity (I) = 30 mW cm<sup>-2</sup>, Total flow rate = 52.5 mL min<sup>-1</sup>, and CO<sub>2</sub> = 400 ppm.

**Detailed correction in the manuscript:**

“pH is an important factor within aqueous chemical reaction processes and is likely to alter the reaction scheme. Yet so far adjusting the pH of particle surfaces is quite tough, and exploring the role of dust surface pH in the reactivity of CO<sub>3</sub><sup>-</sup> is not easily achieved. Notwithstanding, the increase of pH in TiO<sub>2</sub> suspension was observed to promote the production of CO<sub>3</sub><sup>-</sup>, further strengthening the oxidation capability of dust particles. In contrast, decreasing pH is expected to reduce the yield of CO<sub>3</sub><sup>-</sup> since the reaction rate of CO<sub>3</sub><sup>2-</sup> with ·OH is nearly two orders of magnitude higher than that with HCO<sub>3</sub><sup>-</sup>. On this basis, we then examined whether the surface pH of mineral dust can be sustained to maintain fast SO<sub>2</sub> oxidation triggered by CO<sub>3</sub><sup>-</sup> in the typical lifespan of mineral dust. Considering this, we thus plotted the heterogeneous sulfate production over TiO<sub>2</sub> and TiO<sub>2</sub>+CaCO<sub>3</sub> particles versus equivalent exposure time (Fig. S15). Clearly, the sulfate yield builds up steadily during the two-week equivalent exposure time (see more detailed discussion on determining equivalent exposure time in supplementary text 6), suggesting that the regime of CO<sub>3</sub><sup>-</sup> initiated SO<sub>2</sub> oxidation over TiO<sub>2</sub> and TiO<sub>2</sub>+CaCO<sub>3</sub> particles are slightly affected by the possible decrease of surface pH due to accumulation of sulfate production over entire reaction course. In the atmosphere, the lifetime of mineral dust particles ranges from several days to weeks (Bauer and Koch, 2005), and the equivalent exposure time considered in this study (nearly 2 weeks) falls right within the characteristic lifespan range of mineral dust particles. This leads us to deduce that persistent growth of sulfate shows a negligible effect on CO<sub>3</sub><sup>-</sup> initiated SO<sub>2</sub> oxidation scheme proposed in this work.” **(Main Text, Page 14, Line 352-367)**

Other Concerns:

1. The concentrations of  $\text{SO}_2$  used are much higher than the ambient atmospheric concentration.

**Response to Q4:** Thanks for your question. We also note the large gap between the  $\text{SO}_2$  concentration applied in our lab study and the  $\text{SO}_2$  concentration measured in field observations. Therefore, we considered the reaction order of the heterogeneous reaction of  $\text{SO}_2$  on the dust particles  $\text{TiO}_2$ . It follows the pseudo-first-order kinetics in the range of 400 ppb-20000 ppb, covering all  $\text{SO}_2$  concentrations applied in this study. While we note nearly one order of magnitude of  $\text{SO}_2$  concentration gap lies between experimental studies and field observations, we assume this gap may slightly affect the findings in this study, and the proposed mechanism remains valid.

2. Line 228: it is difficult to understand this sentence “ESR data (Fig. 3d) further confirms the increase of  $\text{SO}_3^-$  after 2 min UV irradiation in the presence of carbonate ion” since the change is not very obvious.

**Response to Q5:** We have repeated our ESR measurements to solidify the point that  $\text{SO}_3^-$  is increased in the presence of carbonate radical ions. For visual clarity, we also provided the integrated areas for two ESR spectra. In Fig. R7, the presence of carbonate ions in the  $\text{TiO}_2$ +S(IV) system evidently promotes the generation of  $\text{SO}_3^-$ , which verifies our proposed mechanism.

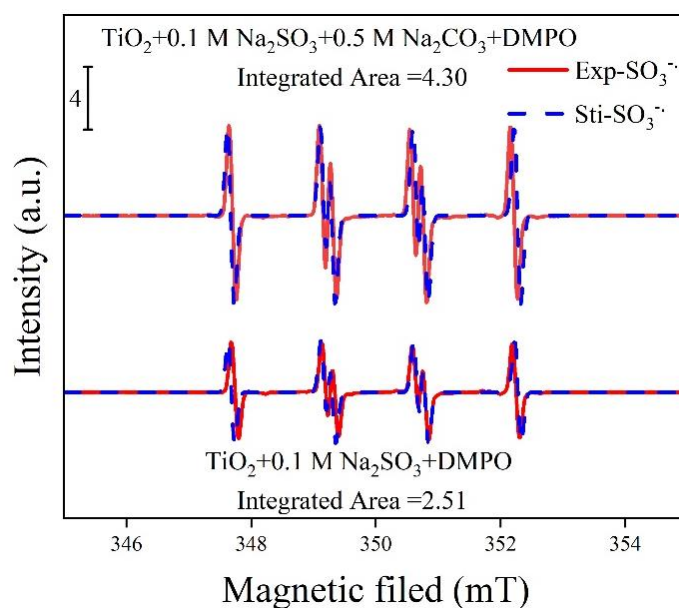


**Fig. R7.** ESR spectrometry of  $[\text{DMPO}-\text{SO}_3^-]$  intermediate formed in a solution of d  $\text{TiO}_2$  (3 mg ~ 4 mL) + 0.1 M  $\text{Na}_2\text{SO}_3$  and  $\text{TiO}_2$  (3 mg ~ 4 mL) + 0.5 M  $\text{Na}_2\text{CO}_3$  + 0.1 M  $\text{Na}_2\text{SO}_3$ . For visual clarity, the integrated areas of ESR profiles were also presented for direct comparison. Exp. and Sti. stand for experimental results and corresponding fitting results using software Isotropic Radicals.

3. Sampling in field observation. The samples collected in daytime and nighttime did not mean they are always in dark and illuminated conditions. The samples collected in nighttime may also have undergone multiple daytime photochemical processes.

**Response to Q6:** Thank you for your thoughtful question. Generally, the aerosol lifetime is on the order of less than an hour to days (Koelemeijer et al., 2006), highly depending on particle size. For example, the lifetime of  $\text{PM}_{10}$  ranges from minutes to hours, and its travel distance, in general, is

less than 10 km (Agustine et al., 2018). When PM downsizes to 2.5  $\mu\text{m}$ ,  $\text{PM}_{2.5}$  has a lifetime prolonged to nearly one day or longer (Liu et al., 2020). Therefore, in our sampling,  $\text{PM}_{3.3}\text{-PM}_{9.0}$  are expected to have a relatively long lifetime, on the order of several hours or more, which enables the heterogeneous reaction process to become a more important contributor to overall sulfate ions measured in  $\text{PM}_{3.3}\text{-PM}_{9.0}$  than that in  $\text{PM}_{\geq 9.0}$ . This is supported by our observations where during the daytime hours the correlation coefficients for  $\text{PM}_{3.3}\text{-PM}_{9.0}$ , i.e. 0.56 (sulfate vs carbonate) and 0.61 (sulfate vs bicarbonate), are higher than that of  $\text{PM}_{\geq 9.0}$ , i.e. 0.489 (sulfate vs carbonate) and 0.36 (sulfate vs bicarbonate), respectively.

We also note that their correlations are not high in part because the concentration of water-soluble ions determined in these samples may not come from the net contribution of processes in day-time and night-time periods. As you mentioned, some undesired processes that take place during the day(nigh)-night(day) shifts may also contribute to the concentration of sulfate ions in separate sampling hours. Nevertheless, the negative correlations between the mass concentrations of sulfate ions and (bi)carbonate ions are observed in the nighttime hours, consistent with the suppression of sulfate formation by  $\text{CO}_2$  in the dark experiments. Instead, positive correlations are seen for those ions within PM sampled during the daytime hours. This matches with the scenarios in which sulfate production upon irradiation in the presence of (bi) carbonate ions is increased over both model and authentic dust particles. Taken the lifetime of  $\text{PM}_{\geq 3.3}$  as well as the distinct trends observed during day-time and night-time periods, it is plausible that in this study the ambient PM collected separately in the daytime and nighttime hours, to some extent, are likely to reflect aerosol particles that mainly go through heterogeneous reaction under dark and irradiation, analogous to the scenario where we considered in lab simulations.

***Detailed correction in the manuscript:***

*“However, under the low wind speed ( $0.76 \pm 0.73$ ), correlation coefficients  $R^2$  obtained for relationship between bi(carbonate) and sulfate ions are not promising, 0.56 (sulfate vs carbonate) and 0.61 (sulfate vs bicarbonate) for  $\text{PM}_{3.3}\text{-PM}_{9.0}$  during daytime hours. A plausible explanation is that although less significant, local primary emission source also brings certain bias and uncertainty to the correlation analysis. Shanghai is a coastal city, and sulfate species such as  $\text{K}_2\text{SO}_4$  and  $\text{Na}_2\text{SO}_4$  from the sea salt contribute to the local sulfate emission as well (Long et al., 2014). On the other hand, this novel  $\text{SO}_2$  oxidation channel is in the infant stage, and only active mineral dust components have been considered in this work whereas other components found in the coarse mode of PM such as organic matter, elemental carbon as well as sea salt (Cheung et al., 2011) are likely to involve this mechanism and alter the response of sulfate yield to  $\text{SO}_2$  heterogeneous uptake. In addition, the concentration of water-soluble ions determined in these samples (relatively small size) may not come from the net contribution of heterogenous reaction processes in absolute day-time and night-time periods. Some of the undesired processes that take place during day(nigh)-night(day) shifts may also contribute to the concentration of sulfate ions in separate sampling hours.”*

***(Main Text, Page 16, Line 413-424)***

4. In addition, as proposed by Sullivan et al. (Atmos. Chem. Phys., 7, 1213–1236, 2007), oxidation of S(IV) to S(VI) by iron in the aluminosilicate dust is a possible explanation for the enrichment of sulphate in Asian mineral dust. So, how to exclude the effect of Fe in this study?

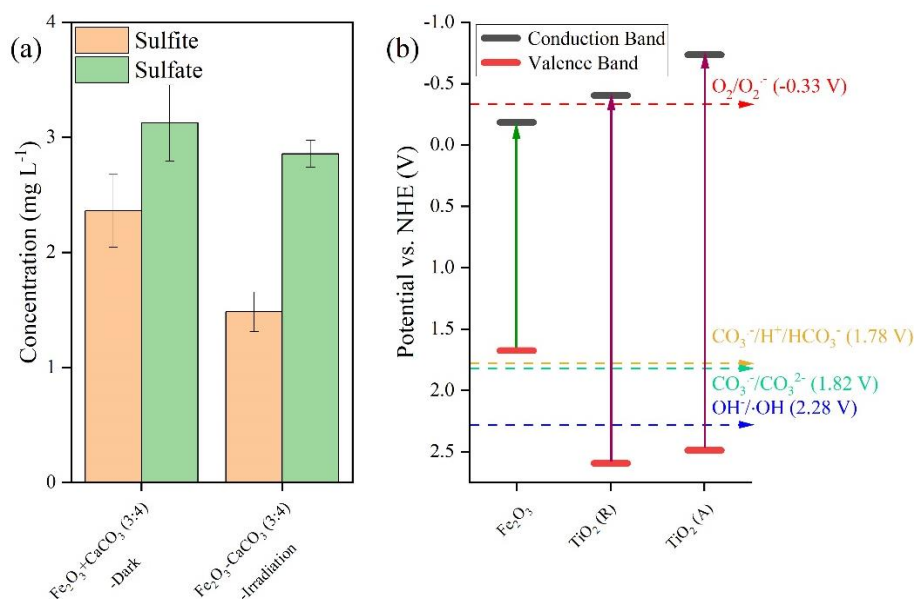


**Fig. R8.** (a) Determination of sulfite and sulfate concentration after exposure to air flow under irradiation in Fe<sub>2</sub>O<sub>3</sub>-CaCO<sub>3</sub> particles for 20 min. (b) Band positions of typical active mineral dust components (at pH = 7 in aqueous media), with highlights on the oxidation capability and generation of reactive oxygen species. Reaction conditions: RH = 30 %, Light intensity (I) = 30 mW cm<sup>-2</sup>, Total flow rate = 52.5 mL min<sup>-1</sup>.

**Response to Q7:** Thanks for your suggestion. We thus considered the role of iron promoters in our proposed mechanism by using the alpha-Fe<sub>2</sub>O<sub>3</sub>+CaCO<sub>3</sub> mixture. Similar to experiments using TiO<sub>2</sub>+CaCO<sub>3</sub> mixture, alpha-Fe<sub>2</sub>O<sub>3</sub>+CaCO<sub>3</sub> are prepared by grinding alpha-Fe<sub>2</sub>O<sub>3</sub> and CaCO<sub>3</sub>. The ratio of iron oxide and calcium components is fixed at 3:4 according to EDS mapping analysis results. In panel a, our results show that alpha-Fe<sub>2</sub>O<sub>3</sub> can not trigger fast SO<sub>2</sub> oxidation in the presence of carbonate ions upon irradiation, which is distinguished from results we derived from the TiO<sub>2</sub>+CaCO<sub>3</sub> mixture. This can be explained by the fact that Fe<sub>2</sub>O<sub>3</sub> shows a lower redox activity compared to TiO<sub>2</sub> regardless of the anatase phase and rutile phase (panel b). We collected the redox potential vs NHE (V) of O<sub>2</sub>/O<sub>2</sub><sup>-</sup>, CO<sub>3</sub><sup>-</sup>/H<sup>+</sup>/HCO<sub>3</sub><sup>-</sup>, and CO<sub>3</sub><sup>-</sup>/CO<sub>3</sub><sup>2-</sup> in the previous literature, with both valence band and conduction band information of each dust particle, i.e. semiconductors, shown in panel a. Owing to the strong redox capability of TiO<sub>2</sub> particles, where the photo-induced electrons and holes are able to form O<sub>2</sub><sup>-</sup> and ·OH radical ions, respectively. In stark contrast, mineral dust component Fe<sub>2</sub>O<sub>3</sub> has a rather narrow band gap, with its valence band and conduct band lying at -0.18 and at 1.68 V vs. NHE at pH = 7, lower than the redox potential required for generating CO<sub>3</sub><sup>-</sup>/H<sup>+</sup>/HCO<sub>3</sub><sup>-</sup>, and CO<sub>3</sub><sup>-</sup>/CO<sub>3</sub><sup>2-</sup>, which thus can not produce CO<sub>3</sub><sup>-</sup>.

Nevertheless, we are aware of the inconsistency between our lab results and the reported results in the literature (Li et al., 2019; Toledano and Henrich, 2001). Toledano et al. observed a UV-induced increase in adsorption of SO<sub>2</sub> over alpha-Fe<sub>2</sub>O<sub>3</sub> (0001) using the XPS technique. The difference is likely to correlate to the different light sources and dust sources. 30 mW cm<sup>-2</sup> of photon flux was applied using a solar simulator in our lab study, corresponding to 0.3 times of AM 1.5 G solar irradiance while they employed a focused 200 W Hg(Xe) lamp, which provides a strong light source, with  $h\nu > E_{\text{gap}}$  (2.2 eV) roughly 70 times of the solar flux in that wavelength range. On the other hand, we adopted commercially available alpha-Fe<sub>2</sub>O<sub>3</sub> nanoparticles and the chemical

properties of which are believed to be different from that of single-crystal  $\text{Fe}_2\text{O}_3$  with a pure (0001) surface. It is believed that crystal plane, morphology, and size can modulate the inherent band gap (the position of conduction band relative to the position of valence band) of semiconductors (Alivisatos, 1996; Xu et al., 2013; Xu et al., 2015). In Li's work, they synthesized four types of  $\text{Fe}_2\text{O}_3$  nanomaterials with different morphologies, which have a various abundance of each crystal facet. This leads to distinct photochemical properties compared to pristine  $\text{Fe}_2\text{O}_3$  nanoparticles.

In addition, we observed a slight decrease of sulfite and sulfate yield upon irradiation compared to dark experiments, consistent with Du's work (Du et al., 2019), in which a more evidently decrease is found in the initial reaction stage. A plausible explanation for this observation is that while we applied xenon lamp as a light source for experiments, elevated temperature in the chamber is likely to decrease the  $\text{SO}_2$  uptake over dust particles, more evidently for those particles with dark colors. Our earlier study shows that  $\text{SO}_2$  uptake over  $\text{Fe}_2\text{O}_3$  particles are sensitive to temperature (Wang et al., 2018), and persistent increase in temperature hinders  $\text{SO}_2$  adsorption, and consequently reduce sulfate yield. Overall, we show that ferric oxide can not initiate fast  $\text{SO}_2$  oxidation by generating  $\text{CO}_3^-$  ions where we considered in this study due to its poor photo activity although ferric chemistry is important in secondary sulfate formation in the atmosphere.

***Detailed correction in the manuscript:***

*“ $\text{Fe}_2\text{O}_3$  is also one of the crucial components found in the authentic mineral dust (El Zein et al., 2013), and it has been reported to produce ROS under solar irradiation (Li et al., 2019), thus likely involving the reaction mechanism proposed in this work. Similar to experiments using  $\text{TiO}_2+\text{CaCO}_3$  mixture,  $\alpha\text{-Fe}_2\text{O}_3+\text{CaCO}_3$  are prepared by grinding  $\alpha\text{-Fe}_2\text{O}_3$  and  $\text{CaCO}_3$ . In Fig. S9a, our results show that  $\alpha\text{-Fe}_2\text{O}_3$  can not trigger fast  $\text{SO}_2$  oxidation in the presence of carbonate ions upon irradiation, which is distinguished from results we derived from the  $\text{TiO}_2+\text{CaCO}_3$  mixture. This can be explained by the fact that  $\text{Fe}_2\text{O}_3$  shows a lower redox activity relative to  $\text{TiO}_2$  (Fig. S9b), where its strong redox capability essentially enables photo-induced electrons and holes to produce  $\text{O}_2^-$  and  $\cdot\text{OH}$  radical ions. In stark contrast, the valence band and conduct band of  $\text{Fe}_2\text{O}_3$  lie at -0.18 and at 1.68 V vs. NHE (pH = 7), lower than the redox potential required for generating  $\text{O}_2^-$ ,  $\cdot\text{OH}$  as well as  $\text{CO}_3^-$  (Li et al., 2016). Hence, no promoted sulfate production is seen for  $\text{Fe}_2\text{O}_3+\text{CaCO}_3$  particles under irradiation. More discussion on the inconsistency between our study and the previous results regarding the response of  $\text{SO}_2$  oxidation to solar irradiation can be found in supplementary text 3.*

*Overall, we show that upon irradiation atmospherically relevant content of  $\text{TiO}_2$  (nearly 1 %) found in authentic dust simulants is able to interact with carbonate ions to launch a fast  $\text{SO}_2$  oxidation channel, which is beyond the conventional regime of alkaline neutralization of  $\text{H}_2\text{SO}_4$ . Unlike  $\text{TiO}_2$ ,  $\alpha\text{-Fe}_2\text{O}_3$  can not initiate fast  $\text{SO}_2$  oxidation by generating  $\text{CO}_3^-$  due to its limited photo activity although ferric chemistry is important in secondary sulfate formation in the atmosphere (Sullivan et al., 2007; Yermakov and Purnal, 2003).”*

**(Main Text, Page 7, Line 173-189)**

5. Conclusion and atmospheric implications: this study only found the enhanced sulfate formation in mixed  $\text{TiO}_2$  and  $\text{CaCO}_3$  particles compared to individual  $\text{TiO}_2$  or  $\text{CaCO}_3$  particles. However, the hypotheses of  $\text{CO}_2^-$  derived carbonate species and carbonate salt works as the precursor of  $\cdot\text{CO}_3^-$  is exaggerated. As seen in this study,  $\text{TiO}_2$  is necessary but its content in atmospheric



particulate matter is very low. Considering the unclear role of  $\bullet\text{CO}_3^-$ , as well as the high concentration of  $\text{SO}_2$  used, its implications even on sulfate formation is limited. Consequently, the extension of its atmospheric implications to fine PM concentration, human health, and climate is not meaningful.

Response to Minor Concern 5: Thanks for your comments. We have performed several experiments to prove the significance of the novel  $\text{SO}_2$  oxidation channel proposed in this work. The detailed discussion is shown as follows:

### 1. $\text{CO}_3^-$ production from the atmospherically-relevant concentration of $\text{CO}_2$

In this work, we investigated not only the synergistic effect between  $\text{CaCO}_3$  and  $\text{TiO}_2$  but the role of atmospheric atmospherically-relevant concentration of  $\text{CO}_2$  in promoting  $\text{SO}_2$  oxidation. By using a series of authentic dust particles such as Arizona test dust (ATD), clays IMt-2 (Illite, Mont., USA), and K-Ga-2 (Kaolin, Georgia, USA), we prove that  $\text{CO}_2$ -derived carbonate radical ions can increase sulfate production, especially for K-Ga-2 due to its enriched  $\text{TiO}_2$  content ( $\approx 3\%$ ). It almost doubles the sulfate yield in the presence of  $\text{CO}_2$ +air upon irradiation compared to that in the air flow upon irradiation. This result indicates that our proposed scheme does exist and plays role in sulfate formation in the atmosphere.

#### ***Detailed correction in the manuscript:***

*“As another step toward a real scenario in the atmosphere, experimental trials employing authentic dust particles, i.e. Arizona test dust (ATD), clays IMt-2 (Illite, Mont., USA) and K-Ga-2 (Kaolin, Georgia, USA), were implemented (Table S2). In Fig. 4, K-Ga-2 clay exhibits the most marked promotional effect on sulfate yield (by nearly 100 % increased sulfate production in the  $\text{CO}_2$ -involved case under irradiation). This correlates with its considerable  $\text{TiO}_2$  contents (3.43 %) in the K-Ga-2 clay, in which active intermediates are readily evolved from  $\text{TiO}_2$  and (bi)carbonate species upon irradiation. However, the promotional effect of  $\text{CO}_2$  on sulfate production under irradiation is weak for IMt-2 (the content of  $\text{TiO}_2 \approx 0.99\%$ ) and ATD (the content of  $\text{TiO}_2 \approx 0.46\%$ ) as compared to K-Ga-2 particles. This may correlate to their higher mass fraction of alkaline earth metal oxide (denoted as A.E.), which enables dust particles to possess a large number of (bi)carbonate species in the natural environment where they have experienced long-term exposure to atmospheric  $\text{CO}_2$  during the regional transport. Therefore, the aforementioned synergetic effect takes effect over IMt-2 and ATD particles even without exposure to  $\text{CO}_2$  due to the presence of abundant carbonate formed, and a less evident increase of sulfate yield is observed.”*

**(Main Text, Page 8, Line 200-210)**

### 2. Observation of enhanced sulfate formation over synthetic mineral dust proxy ( $\text{SiO}_2$ : $\text{Al}_2\text{O}_3$ : $\text{CaCO}_3$ : $\text{TiO}_2 = 81:9.6:7.7:1.0$ )

*“To generalize our finding to a more real condition, the rapid  $\text{SO}_2$  oxidation pathway was further probed by employing mineral dust simulants where two dominant crust constituents  $\text{SiO}_2$  and  $\text{Al}_2\text{O}_3$  were introduced into  $\text{TiO}_2$ - $\text{CaCO}_3$  particles to mimic the authentic mineral dust particles in the atmosphere, with specific component and corresponding ratio information shown in Table S1. It is worth mentioning that the determination of the ratio of each component in the simulants relies on the EDS mapping results of ATD particles. In Fig. 2, the introduction of  $\text{TiO}_2$  components ( $\approx 1\%$  wt.) into  $\text{SiO}_2$ - $\text{Al}_2\text{O}_3$  leads to 81.6 % enhancement of sulfate production while merely 24.8 % wt. increase of sulfate yield was observed once  $\approx 8\%$  wt. of  $\text{CaCO}_3$  was incorporated into  $\text{SiO}_2$ - $\text{Al}_2\text{O}_3$*



dust particles. Surprisingly, mixing of  $\approx 1$  % mass fraction of  $\text{TiO}_2$  and  $\approx 8$  % wt. of  $\text{CaCO}_3$  into  $\text{SiO}_2\text{-Al}_2\text{O}_3$  gives rise to a 235 % increase of sulfate formation relative to that of  $\text{SiO}_2\text{-Al}_2\text{O}_3$ . Hence, the synergistic effect on heterogeneous oxidation of  $\text{SO}_2$  is likely to take effect in the atmosphere. Overall, we show that even using the mass ratio of  $\text{SiO}_2$ ,  $\text{Al}_2\text{O}_3$ ,  $\text{CaCO}_3$ , and  $\text{TiO}_2$  detected in authentic particles, evident acceleration of sulfate production is observed. Hence, the proposed mechanism in this study is prone to play role in the atmosphere.” (Main Text, Page 8, Line 164-173)

### 3. Investigation of the reaction order of $\text{SO}_2$ uptake over dust particles ( $\text{SO}_2$ concentration ranges from 400 ppb to 20000 ppb)

We note that a relatively high concentration of  $\text{SO}_2$  is applied for experiments in this work, and this concentrate gap may bring uncertainty to the reaction kinetics and applicability of the proposed reaction scheme in the atmosphere. To properly describe the reaction efficiency of gas-surface interactions, sulfate formation rates as a function of  $\text{SO}_2$  concentration were initially determined to verify its reaction order in the selected concentration range (Fig. S10 A-E), which is a crucial step to give a credible estimation of  $\text{SO}_2$  uptake coefficient. Based on a prior study (Shang et al., 2010b),  $\text{SO}_2$  uptake on particle surfaces depends on the  $\text{SO}_2$  concentrations and active sites, which thus could be described by the following equation (Eq. R6):

$$\frac{d[\text{SO}_4^{2-}]}{dt} = k[\text{SO}_2]^m[\text{CO}_2]^l[\text{TiO}_2]^n[\text{H}_2\text{O}]^p \quad \text{[R6]}$$

where  $[\text{SO}_4^{2-}]$  refers to the sulfate concentration on  $\text{TiO}_2$  surfaces,  $[\text{SO}_2]$ (  $[\text{CO}_2]$ ) to  $\text{SO}_2$  ( $\text{CO}_2$ ) gas concentration employed in the system,  $[\text{TiO}_2]$  to the concentration of active sites on the  $\text{TiO}_2$  particle surfaces, and  $[\text{H}_2\text{O}]$  represents for surface water concentration, and  $m$ ,  $l$ ,  $n$ , and  $p$  are the reaction orders of corresponding species. Clearly, the steady growth of sulfate on  $\text{TiO}_2$  particles in the presence of  $9.83 \times 10^{15}$  molecules  $\text{cm}^{-3}$   $\text{CO}_2$  made a clear indication (panel A-E) that the decrease in surface active sites is negligible. Meanwhile, mass flow controllers provide stable gas flow and maintain the constant concentrations of humidified air and  $\text{CO}_2$ , which allows us to simplify the Eq. R6 to Eq. R7 through a logarithm function.

$$\lg \frac{d[\text{SO}_4^{2-}]}{dt} = \lg k + m \lg [\text{SO}_2] + C \quad \text{[R7]}$$

where  $C$  stands for  $l \lg [\text{TiO}_2] + n \lg [\text{TiO}_2] + p \lg [\text{H}_2\text{O}]$ , and  $[\text{SO}_2]$  for the concentration of  $\text{SO}_2$  where particles are exposed. We then plotted the sulfate formation rate against exposed  $\text{SO}_2$  concentration. Linear fitting analysis for those points resulted in 1.13 order for the reaction, with  $R^2 \approx 0.99$  (Fig. S10 F). So far, 400 ppb is the lowest concentration that we are able to apply for the uptake measurements due to the limitation of the current experimental setup. The prior work has demonstrated that atmospheric  $\text{SO}_2$  concentration reaches up to 40 ppb (Franchin et al., 2015). We note that a difference of nearly a factor of 10 remains for the  $\text{SO}_2$  concentration employed in laboratory studies and that measured in field observations. Nevertheless, we have already verified its pseudo-first-order kinetic in the wide range of 400-20000 ppb. This leads us to assume that uptake coefficients estimated under ppm level remain valid, and those datasets derived from laboratory chambers are able to be generalized to the atmosphere condition. (Supporting Information, Page S5)

#### 4. Observation of the ejection of gas-phase $\text{CO}_3^-$ on the dust particle surface upon irradiation.

Through probe molecular aniline, we determined the steady concentration of  $[\cdot\text{OH}]_{\text{ss}}$  and  $[\text{CO}_3^-]_{\text{ss}}$  released from  $\text{TiO}_2$  particles in the absence and presence of  $\text{CO}_2$ , respectively. Specifically, the steady-state concentration of carbonate radicals was determined to be  $1.39 \times 10^{-13}$  M for the  $\text{TiO}_2+\text{Air}+\text{CO}_2$  system, which is much higher than that of hydroxyl radicals measured in the  $\text{TiO}_2+\text{Air}$  system ( $2.15 \times 10^{-15}$  M). Previously, it has been demonstrated that the gas-phase hydroxyl radical produced from  $\text{TiO}_2$  has a great impact on sulfate formation. Our study unfolds that the production of gas-phase carbonate radical ions in the presence of  $\text{CO}_2$  over mineral dust upon irradiation. To be important, since  $\text{CO}_3^-$  enter into the gas phase, they will promote the oxidation of  $\text{SO}_2$  in the gas phase to form external sulfate aerosol, which is known to serve as cloud condensation nuclei and play a role in the global climate by scattering solar radiation. Hence, the rapid  $\text{SO}_2$  oxidation pathway proposed in this work shows its non-negligible atmospheric implications to fine PM concentration, human health, and climate.

##### ***Detailed correction in the manuscript:***

*“When  $\text{CO}_2$  (atmospheric relevant concentration) is introduced into the home-made flow-cell chamber, with an intervening gap between  $\text{TiO}_2$ -coated film and probe molecule solution fixing at nearly 2 mm, and a short distance of which allows possible gaseous ROS to diffuse and react with aniline molecular (None, 2013). An increased degradation rate of aniline was seen, which can be attributed to the generation of active carbonate radical ions (Fig. S17). The maximum concentration of steady-state  $\text{CO}_3^-$  radical ions supplied by partition processes between gas phase and solid-liquid phases (humified dust particles) was determined to be  $1.39 \times 10^{-13}$  M for the  $\text{TiO}_2+\text{Air}+\text{CO}_2$  system, which is over one order of magnitudes higher than that of  $\cdot\text{OH}$  for  $\text{TiO}_2+\text{Air}+\text{system}$  ( $2.15 \times 10^{-15}$  M). This observation matches with the earlier study where the concentration of carbonate radical can be two orders of magnitudes than  $\cdot\text{OH}$  over the water surface (Sulzberger et al., 1997a).”*  
**(Supporting Information, Page 15, Line 373-380).**

##### **Reference:**

- Agustine I, Yulinawati H, Gunawan D, Suswanto E: Potential impact of particulate matter less than 10 micron ( $\text{PM}_{10}$ ) to ambient air quality of Jakarta and Palembang. *Iop C Ser Earth Env*, 106 <https://doi.org/10.1088/1755-1315/106/1/012057>, 2018.
- Ali SZ, Kanao F, Takehiro M, Joichi S: Quantitative Estimation of Adsorbed Water Layer on Austenitic Stainless Steel. *Tribology Online*, 10,314-319, <https://doi.org/10.2474/trol.10.314>, 2015.
- Alivisatos AP: Semiconductor clusters, nanocrystals, and quantum dots. *Science*, 271,933-937, <https://doi.org/10.1126/science.271.5251.933>, 1996.
- Baltrusaitis J, Schuttlefield J, Zeitler E, Grassian VH: Carbon dioxide adsorption on oxide nanoparticle surfaces. *Chem. Eng. J.*, 170,471-481, <https://doi.org/10.1016/j.cej.2010.12.041>, 2011.
- Bauer SE, Koch D: Impact of heterogeneous sulfate formation at mineral dust surfaces on aerosol loads and radiative forcing in the Goddard Institute for Space Studies general circulation model. *J. Geophys. Res.*, 110 <https://doi.org/10.1029/2005jd005870>, 2005.
- Behrman EJ: Degradation kinetics and mechanism of aniline by heat-assisted persulfate oxidation *Comment. J. Environ. Sci. China*, 64,352-352, 10.1016/j.jes.2018.02.008, 2018.
- Chavadej S, Phuaphromyod P, Gulari E, Rangsunvigit P, Sreethawong T: Photocatalytic degradation of 2-propanol by using  $\text{Pt/TiO}_2$  prepared by microemulsion technique. *Chem. Eng. J.*, 137,489-

- 495, <https://doi.org/10.1016/j.cej.2007.05.001>, 2008.
- Chen Y, Tong SR, Li WR, Liu YP, Tan F, Ge MF, et al.: Photocatalytic Oxidation of SO<sub>2</sub> by TiO<sub>2</sub>: Aerosol Formation and the Key Role of Gaseous Reactive Oxygen Species. *Environ. Sci. Technol.*, 55,9784-9793, <https://doi.org/10.1021/acs.est.1c01608>, 2021.
- Cheung K, Daher N, Kam W, Shafer MM, Ning Z, Schauer JJ, et al.: Spatial and temporal variation of chemical composition and mass closure of ambient coarse particulate matter (PM<sub>10-2.5</sub>) in the Los Angeles area. *Atmos. Environ.*, 45,2651-2662, <https://doi.org/10.1016/j.atmosenv.2011.02.066>, 2011.
- Cwiertny DM, Young MA, Grassian VH: Chemistry and photochemistry of mineral dust aerosol. *Annu. Rev. Phys. Chem.*, 59,27-51, <https://doi.org/10.1146/annurev.physchem.59.032607.093630>, 2008.
- Czapski G, Lyman SV, Schwarz HA: Acidity of the carbonate radical. *J. Phys. Chem. A*, 103,3447-3450, <https://doi.org/10.1021/jp984769y>, 1999.
- Du C, Kong L, Zhanzakova A, Tong S, Yang X, Wang L, et al.: Impact of adsorbed nitrate on the heterogeneous conversion of SO<sub>2</sub> on  $\alpha$ -Fe<sub>2</sub>O<sub>3</sub> in the absence and presence of simulated solar irradiation. *Sci. Total. Environ.*, 649,1393, <https://doi.org/10.1016/j.scitotenv.2018.08.295>, 2019.
- Dupart Y, King SM, Nekat B, Nowak A, Wiedensohler A, Herrmann H, et al.: Mineral dust photochemistry induces nucleation events in the presence of SO<sub>2</sub>. *Proc. Natl. Acad. Sci. USA*, 109,20842-20847, <https://doi.org/10.1073/pnas.1212297109>, 2012.
- Duran A, Monteagudo JM, Martin IS, Merino S, Chen X, Shi X: Solar photo-degradation of aniline with rGO/TiO<sub>2</sub> composites and persulfate. *Sci. Total. Environ.*, 697,134086-, <https://doi.org/10.1016/j.scitotenv.2019.134086>, 2019.
- El Zein A, Romanias MN, Bedjanian Y: Kinetics and Products of Heterogeneous Reaction of HONO with Fe<sub>2</sub>O<sub>3</sub> and Arizona Test Dust. *Environ. Sci. Technol.*, 47,6325-6331, <https://doi.org/10.1021/es400794c>, 2013.
- Franchin A, Ehrhart S, Leppa J, Nieminen T, Gagne S, Schobesberger S, et al.: Experimental investigation of ion-ion recombination under atmospheric conditions. *Atmos. Chem. Phys.*, 15,7203-7216, <https://doi.org/10.5194/acp-15-7203-2015>, 2015.
- Gao J, Meng YQ, Benton A, He J, Jacobsohn LG, Tong JH, et al.: Insights into the Proton Transport Mechanism in TiO<sub>2</sub> Simple Oxides by In Situ Raman Spectroscopy. *ACS Appl. Mater. Inter.*, 12,38012-38018, [10.1021/acsami.0c08120](https://doi.org/10.1021/acsami.0c08120), 2020.
- Jiang HT, Liu YC, Xie Y, Liu J, Chen TZ, Ma QX, et al.: Oxidation Potential Reduction of Carbon Nanomaterials during Atmospheric-Relevant Aging: Role of Surface Coating. *Environ. Sci. Technol.*, 53,10454-10461, <https://doi.org/10.1021/acs.est.9b02062>, 2019.
- Kansal SK, Singh M, Sud D: Studies on TiO<sub>2</sub>/ZnO photocatalysed degradation of lignin. *J. Hazard Mater.*, 153,412-417, <https://doi.org/10.1016/j.jhazmat.2007.08.091>, 2008.
- Koelemeijer R, Homan CD, Matthijsen J: Comparison of spatial and temporal variations of aerosol optical thickness and particulate matter over Europe. *Atmos. Environ.*, 40,5304-5315, <https://doi.org/10.1016/j.atmosenv.2006.04.044>, 2006.
- Li KJ, Kong LD, Zhanzakova A, Tong SY, Shen JD, Wang T, et al.: Heterogeneous conversion of SO<sub>2</sub> on nano  $\alpha$ -Fe<sub>2</sub>O<sub>3</sub>: the effects of morphology, light illumination and relative humidity. *Environ. Sci. Nano.*, 6,1838-1851, <https://doi.org/10.1039/c9en00097f>, 2019.
- Li X, Yu J, Jaroniec M: Hierarchical photocatalysts. *Chem. Soc. Rev.*, 45,2603-2636, <https://doi.org/10.1039/c5cs00838g>, 2016.

- Liu Y, Wang T, Fang X, Deng Y, Cheng H, Fu H, et al.: Impact of greenhouse gas CO<sub>2</sub> on the heterogeneous reaction of SO<sub>2</sub> on Alpha-Al<sub>2</sub>O<sub>3</sub>. *Chinese Chem. Lett.*, <https://doi.org/10.1016/j.cclet.2020.04.037>, 2020.
- Long SL, Zeng JR, Li Y, Bao LM, Cao LL, Liu K, et al.: Characteristics of secondary inorganic aerosol and sulfate species in size-fractionated aerosol particles in Shanghai. *J. Environ. Sci. China*, 26,1040-1051, [https://doi.org/10.1016/S1001-0742\(13\)60521-5](https://doi.org/10.1016/S1001-0742(13)60521-5), 2014.
- Mogili PK, Kleiber PD, Young MA, Grassian VH: Heterogeneous uptake of ozone on reactive components of mineral dust aerosol: an environmental aerosol reaction chamber study. *J. Phys. Chem. A*, 110,13799-807, <https://doi.org/10.1021/jp063620g>, 2006.
- Nanayakkara CE, Larish WA, Grassian VH: Titanium Dioxide Nanoparticle Surface Reactivity with Atmospheric Gases, CO<sub>2</sub>, SO<sub>2</sub>, and NO<sub>2</sub>: Roles of Surface Hydroxyl Groups and Adsorbed Water in the Formation and Stability of Adsorbed Products. *J. Phys. Chem. C*, 118,23011-23021, 2015.
- Nguyen XQ, Broz Z, Uchytel P, Nguyen QT: Methods for the Determination of Transport Parameters of Gases in Membranes. *J. Chem. Soc. Faraday T.*, 88,3553-3560, <https://doi.org/10.1039/FT9928803553>, 1992.
- None: In-Situ Characterization of Heterogeneous Catalysts. *Focus on Catal.*, 2013,8, [https://doi.org/10.1016/S1351-4180\(13\)70477-X](https://doi.org/10.1016/S1351-4180(13)70477-X), 2013.
- Peters SJ, Ewing GE: Water on Salt: An Infrared Study of Adsorbed H<sub>2</sub>O on NaCl (100) under Ambient Conditions. *J. Phys. Chem. B*, 101,10880-10886, <https://doi.org/https://doi.org/10.1021/jp972810b>, 1997.
- Ruiz-Agudo E, Kudlacz K, Putnis CV, Putnis A, Rodriguez-Navarro C: Dissolution and Carbonation of Portlandite [Ca(OH)<sub>2</sub>] Single Crystals. *Environ. Sci. Technol.*, 47,11342-11349, <https://doi.org/10.1021/es402061c>, 2013.
- Samuni A, Goldstein S, Russo A, Mitchell JB, Krishna MC, Neta P: Kinetics and mechanism of hydroxyl radical and OH-adduct radical reactions with nitroxides and with their hydroxylamines. *J. Am. Chem. Soc.*, 124,8719-8724, <https://doi.org/10.1021/ja017587h>, 2002.
- Shang J, Li J, Zhu T: Heterogeneous reaction of SO<sub>2</sub> on TiO<sub>2</sub> particles. *Sci. China Chem.*, 53,2637-2643, <https://doi.org/10.1007/s11426-010-4160-3>, 2010a.
- Shang J, Li J, Zhu T: Heterogeneous reaction of SO<sub>2</sub> on TiO<sub>2</sub> particles. *Sci. China Chem.*, 2637-2643, <https://doi.org/10.1007/s11426-010-4160-3>, 2010b.
- Sullivan RC, Guazzotti SA, Sodeman DA, Prather KA: Direct observations of the atmospheric processing of Asian mineral dust. *Atmos. Chem. Phys.*, 7,1213-1236, <https://doi.org/10.5194/acp-7-1213-2007>, 2007.
- Sulzberger B, Canonica S, Egli T, Giger W, Klausen J, Gunten Uv: Oxidative transformations of contaminants in natural and in technical systems. *Chimia*, 51,900-907, <https://doi.org/10.1051/epjconf/20101105003>, 1997a.
- Sulzberger B, Canonica S, Egli T, Giger W, Klausen J, von Gunten U: Oxidative transformations of contaminants in natural and in technical systems. *Chimia*, 51,900-907, <https://doi.org/10.1051/epjconf/20101105003>, 1997b.
- Sun P, Tyree C, Huang CH: Inactivation of Escherichia coli, Bacteriophage MS2, and Bacillus Spores under UV/H<sub>2</sub>O<sub>2</sub> and UV/Peroxydisulfate Advanced Disinfection Conditions. *Environ. Sci. Technol.*, 50,4448-4458, <https://doi.org/10.1021/acs.est.5b06097>, 2016.
- Tang WZ, An H: Uv/TiO<sub>2</sub> Photocatalytic Oxidation of Commercial Dyes in Aqueous-Solutions.

- Chemosphere, 31,4157-4170, [https://doi.org/10.1016/0045-6535\(95\)80015-D](https://doi.org/10.1016/0045-6535(95)80015-D), 1995.
- Toledano DS, Henrich VE: Kinetics of SO<sub>2</sub> adsorption on photoexcited alpha-Fe<sub>2</sub>O<sub>3</sub>. Journal of Physical Chemistry B, 105,3872-3877, <https://doi.org/10.1021/jp003327v>, 2001.
- Wang T, Liu YY, Deng Y, Fu HB, Zhang LW, Chen JM: The influence of temperature on the heterogeneous uptake of SO<sub>2</sub> on hematite particles. Sci.Total. Environ., 644,1493-1502, <https://doi.org/10.1016/j.scitotenv.2018.07.046>, 2018.
- Wang XM, Huang X, Zuo CY, Hu HY: Kinetics of quinoline degradation by O<sub>3</sub>/UV in aqueous phase. Chemosphere, 55,733-741, <https://doi.org/10.1016/j.chemosphere.2003.11.019>, 2004.
- Xu H, Ouyang SX, Li P, Kako T, Ye JH: High-Active Anatase TiO<sub>2</sub> Nanosheets Exposed with 95% {100} Facets Toward Efficient H<sub>2</sub> Evolution and CO<sub>2</sub> Photoreduction. ACS Appl. Mater. Inter., 5,1348-1354, <https://doi.org/10.1021/am302631b>, 2013.
- Xu QL, Yu JG, Zhang J, Zhang JF, Liu G: Cubic anatase TiO<sub>2</sub> nanocrystals with enhanced photocatalytic CO<sub>2</sub> reduction activity. Chem. Commun., 51,7950-7953, <https://doi.org/10.1039/c5cc01087j>, 2015.
- Yan JF, Peng JL, Lai LD, Ji FZ, Zhang YH, Lai B, et al.: Activation CuFe<sub>2</sub>O<sub>4</sub> by Hydroxylamine for Oxidation of Antibiotic Sulfamethoxazole. Environ. Sci. Technol., 52,14302-14310, <https://doi.org/10.1021/acs.est.8b03340>, 2018.
- Yermakov AN, Purmal AP: Iron-catalyzed oxidation of sulfite: From established results to a new understanding. Prog. React. Kinet. Mec., 28,189-255, <https://doi.org/10.3184/007967403103165503>, 2003.